

**Blue phosphorescent organic  
light-emitting devices utilizing  
cesium–carbonate-doped  
2,4,6-tris(2',4'-difluoro-[1,1'-  
biphenyl]-4-yl)-1,3,5-triazine**

James S. Swensen  
James E. Rainbolt  
Liang Wang  
Phillip K. Koech  
Evgueni Polikarpov  
Asanga B. Padmaperuma  
Daniel J. Gaspar

# Blue phosphorescent organic light-emitting devices utilizing cesium–carbonate-doped 2,4,6-tris(2',4'-difluoro-[1,1'-biphenyl]-4-yl)-1,3,5-triazine

James S. Swensen, James E. Rainbolt, Liang Wang, Phillip K. Koech, Evgueni Polikarpov, Asanga B. Padmaperuma, and Daniel J. Gaspar  
Pacific Northwest National Laboratory, Energy and Environment Directorate, Richland,  
Washington 99352  
[Daniel.Gaspar@pnl.gov](mailto:Daniel.Gaspar@pnl.gov)

**Abstract.** We report an alternative, high-yielding synthesis for the known compound 2,4,6-tris(2',4'-difluoro-[1,1'-biphenyl]-4-yl)-1,3,5-triazine (tris-(dFB)Tz). The energy of the lowest unoccupied molecular orbital ( $E_{LUMO}$ ) for tris-(dFB)Tz is estimated to be  $-3.5$  eV from electrochemical measurements. The deep  $E_{LUMO}$  of tris-(dFB)Tz affords a material with excellent electron acceptor characteristics for use in  $n$ -doped electron transport layers. Tris-(dFB)Tz shows a four order of magnitude increase in the number of carriers on doping with 8 wt. %  $Cs_2CO_3$ . Enhanced electron injection was also observed on doping with  $Cs_2CO_3$ , which eliminated the necessity for a separate LiF electron injection layer. Blue phosphorescent organic light-emitting devices (OLEDs) were fabricated using  $n$ -doped tris-(dFB)Tz electron transport layers. OLEDs with thick (700-Å)  $Cs_2CO_3$ -doped tris-(dFB)Tz electron transport layers had lower operating voltages than OLEDs with an undoped electron transport layer of bis(diphenylphosphoryl)dibenzothiophene (PO15), which has previously been used in low-voltage, high-efficiency OLEDs. The tris-(dFB)Tz results indicate that aromatic substituted triazines may be promising materials for use as electron acceptors in  $n$ -doped organic electronic systems. © 2011 Society of Photo-Optical Instrumentation Engineers (SPIE). [DOI: [10.1117/1.3528003](https://doi.org/10.1117/1.3528003)]

**Keywords:**  $p$ - $i$ - $n$  organic light-emitting devices; doping; phosphorescence; cesium carbonate; triazine.

Paper 10158SSPR received Aug. 31, 2010; revised manuscript received Oct. 29, 2010; accepted for publication Nov. 03, 2010; published online Jan. 20, 2011.

## 1 Introduction

Organic light-emitting devices (OLEDs) have found application in flat-panel displays and are currently being developed as an energy-efficient lighting technology. Energy efficiency is a function of light output, current, and operating voltage. A direct strategy to increase OLED power efficiency is through reduction of the operating voltage. One common approach to reduce the operating voltage of organic electronic/optoelectronic devices is by doping the transport layers with atoms or molecules that donate charge carriers to the organic transport layer. Several existing reviews detail the progress and understanding of doped organic systems.<sup>1–4</sup> Doping can have two effects: alteration of the bulk conductivity of the material and/or charge injection at the organic material-electrode interface. Bulk doping leads to a higher concentration of free charges (either holes or electrons) in the doped transport layer. Because conductivity is the product of a number of charges and charge mobility, the increase in the number of free charges in the bulk of the transport layer significantly increases its bulk conductivity. The voltage drop across a doped transport layer is reduced due to the higher bulk conductivity. Interfacial doping results from the development of a thin space-charge region within the doped transport layer near the electrode.

This effectively reduces the Schottky barrier, leading to more facile charge injection. This can lead to the formation of an ohmic contact (i.e., barrier free) between the organic semiconductor and the electrode. The overall result of enhanced charge injection at the contact and lower voltage drop across the bulk of the transport layer is a decreased OLED operating voltage.

This paper focuses on electron (*n*)-doped electron transport layers (ETLs). The first report of an *n*-doped ETL in OLEDs was tris(8-hydroxyquinoline) aluminum (Alq3) where Li, Sr, and Sm were used as the *n*-dopants.<sup>5</sup> A charge transfer reaction took place between the reactive metals and Alq3, introducing free electrons into the transport material and increasing its conductivity. Soon thereafter, *n*-doped ETLs using 9-dimethyl-4,7-diphenyl-1,10-phenanthroline (BCP) as the matrix and Li as the dopant were demonstrated,<sup>6,7</sup> followed by 4,7-diphenyl-1,10-phenanthroline (BPhen) doped with Li (Ref. 8) or Cs (Ref. 9). Since then, Cs-doped BPhen has been used extensively in green, red, and white OLEDs due to its high electron mobility and hole-blocking characteristics as well as a triplet energy suitable for green and red phosphorescence. The use of Cs as an *n*-dopant has also been extended to the electron transport materials (ETMs) phenyldipyrenylphosphine oxide (PoPy) (Ref. 10) and tetra-2-pyridinylpyrazine (TPP) (Ref. 11).

Handling and deposition of the alkali metals used as *n*-dopants can be problematic. For which reason, researchers found that salts of alkali metals also function as *n*-dopants. Cs<sub>2</sub>CO<sub>3</sub> was the first alkali metal salt used as an *n*-dopant in OLEDs, as demonstrated by Canon for their proprietary<sup>12</sup> ETm C-ETM. Cs<sub>2</sub>CO<sub>3</sub> was then used to dope Alq3 (Ref. 13), BCP (Ref. 14), and BPhen (Refs. 15 and 16). BPhen has since been used as the ETm with various other salts including RbCO<sub>3</sub> (Refs. 17 and 18), CsF (Ref. 16), and LiQ (Refs. 19 and 20). LiF has been shown<sup>21,22</sup> to work as an *n*-dopant with Alq3. Novaled<sup>TM</sup> demonstrated *n*-doping using their proprietary<sup>23</sup> ETm NET-5 and molecular *n*-dopant NDN-1.

To summarize, ETMs that have been demonstrated in *n*-doped ETLs are limited to Alq3, BCP, BPhen, PoPy, TPP, C-ETM, and NET-5. In this paper, we introduce the compound 2,4,6-tris(2',4'-difluoro-[1,1'-biphenyl]-4-yl)-1,3,5-triazine, tris-(dFB)Tz, an aromatic substituted triazine electron transport material with a deep lowest unoccupied molecular orbit (LUMO) suitable for *n*-doping. This is the first report of *n*-doping tris-(dFB)Tz as well as the first report of the use of tris-(dFB)Tz as the ETL in an OLED. We show that Cs<sub>2</sub>CO<sub>3</sub> effectively dopes tris-(dFB)Tz, increasing the number of carriers by more than four orders of magnitude. Doping tris-(dFB)Tz with Cs<sub>2</sub>CO<sub>3</sub> leads to lower operating voltages than for OLEDs with undoped tris-(dFB)Tz.

## 2 Experiments

Electron-only devices and OLEDs were fabricated on ITO-covered glass purchased from Colorado Concept Coatings LLC (Loveland, CO). Prior to use, these substrates were cleaned in a sequential series of solvents. First, the substrates were soaked in hot isopropanol and trichloroethylene and then sonicated in acetone, and 2-propanol. The substrates were then dried with flowing nitrogen and treated with UV ozone [(UVO)-Cleaner, Jelight Co. (Irvine, CA), 15 mW/cm<sup>2</sup> for 20] min as a final cleaning step. The substrates were then loaded into a nitrogen glove box (<1 ppm H<sub>2</sub>O, <1 ppm O<sub>2</sub>) coupled to a multichamber vacuum deposition system. Organic layers were sequentially deposited onto the ITO-coated substrates by thermal evaporation from tantalum boats in a high vacuum chamber with a base pressure below  $3 \times 10^{-7}$  Torr. Cathodes were defined by thermally depositing a 10-Å thick layer of LiF immediately followed by a 1000-Å-thick layer of Al through a shadow mask with 1-mm-diameter circular openings. Quartz crystal oscillators were used to monitor the thicknesses of the thin films, which were calibrated *ex situ* using ellipsometry or profilometry.

The optical and electrical characteristics of the devices were determined in air, with electrical contact made via a tungsten probe tip on the ITO anode and a 0.002-in.-diam gold wire directly probing the Al cathode. Current–voltage characteristics were measured with an Agilent Technologies (Santa Clara, CA) 4155B semiconductor parameter analyzer. The light output was

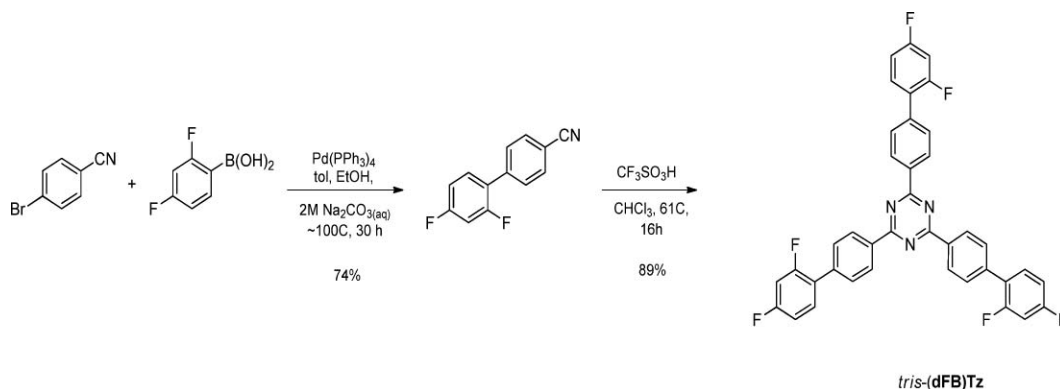


**Fig. 1** Synthesis of *tris*-(dFB)Tz.

detected using a 1-cm<sup>2</sup> Si photodetector placed behind the OLED, which was connected to a Newport (Irvine, CA) multifunction optical meter.

Electrochemical measurements were carried out using Princeton Applied Research (Oak Ridge, TN) potentiostat model 263A with a silver wire as the pseudoreference electrode, a Pt wire as the counter electrode, and glassy carbon as the working electrode. *N,N*-dimethylformamide (DMF) was used as a solvent for reduction potential measurements. Oxidation potentials were measured in dichloromethane distilled over CaH<sub>2</sub>. Tetrabutylammonium hexafluorophosphate was used as a supporting electrolyte. UV-visible (UV-Vis) absorption spectra were collected on a Varian (Santa Clara, CA) Cary 5 UV-Vis-NIR spectrophotometer. The LUMO energy levels were estimated from solution electrochemical reduction potentials.<sup>24</sup> The highest occupied molecular orbital (HOMO) levels were estimated from electrochemical oxidation potentials or the optical bandgap, where electrochemical measurements were not feasible. The triplet energies were obtained from delayed photoluminescence measurements<sup>25</sup> in CH<sub>2</sub>Cl<sub>2</sub> at 77 K. Computations were performed using NWChem, a computational chemistry package for parallel computers, version 5.1 (2007), which was developed by the High Performance Computational Chemistry Group at Pacific Northwest National Laboratory (Richland, WA).<sup>26,27</sup>

### 3 Synthesis and Characterization of *Tris*-(dFB)Tz

#### 3.1 Synthesis *Tris*-(dFB)Tz

*Tris*-(dFB)Tz (Ref. 28) is synthesized easily in two steps from commercially available materials (the scheme in Fig. 1). Although the literature synthesis of this compound begins with the trimerization of 4-bromobenzonitrile to the tri(4-bromophenyl)triazine followed by threefold Suzuki coupling with 2,4-difluorophenylboronic acid, we found that reversing the synthetic sequence results in a simpler, cleaner synthesis. Thus, 4-bromobenzonitrile and 2,4-difluorophenylboronic acid are first coupled under Suzuki conditions to yield the biphenyl compound 1 in good yield. Compound 1 is then trimerized with triflic acid in refluxing (~60°C) chloroform to yield the desired compound very cleanly and in high yields. While the room-temperature trimerization of similar aryl nitriles to 1,3,5-triazines using triflic acid is known,<sup>29,30</sup> heating is required to trimerize compound 1. The syntheses of pyridyl analogs of *tris*-(dFB)Tz were also attempted; however, numerous trimerization reaction conditions failed to give the desired compounds.

##### 3.1.1 2',4'-difluoro-[1,1'-biphenyl]-4-carbonitrile (1)

We combined 4-bromobenzonitrile (5.0 g, 2.8 × 10<sup>-2</sup> mol), 2,4-difluorophenylboronic acid (5.1 g, 3.2 × 10<sup>-2</sup> mol) and tetrakis(triphenylphosphine) palladium(0) (0.5 g, 4.3 × 10<sup>-4</sup> mol) in a round-bottom flask and flushed with argon three times. To this was added a degassed

**Table 1** Photophysical and electrochemical properties of tris-(dFB)Tz.

Compound	Experimental			Computational <sup>d</sup>			
	$\lambda_{\max}$ (nm)	$E_g$ (eV)	$E_{1/2}^{\text{red}}$ (V) <sup>a</sup>	$E_{\text{LUMO}}$ (eV) <sup>b</sup>	$E_{\text{HOMO}}$ (eV) <sup>c</sup>	$E_{\text{LUMO}}$ (eV)	$E_{\text{HOMO}}$ (eV)
tris-(dFB)Tz	305	3.66	1.94	−3.52	− <sup>e</sup>	−2.01	−6.45

<sup>a</sup>First half-electron reduction potential in dichloromethane, with respect to ferrocene/ferrocenium.

<sup>b</sup> $E_{\text{LUMO}} = -5.47 - E_{\text{red}}$ .

<sup>c</sup> $E_{\text{HOMO}} = E_{\text{LUMO}} - E_g$ .

<sup>d</sup>NWChem prediction, B3LYP/6–31G\*.

<sup>e</sup>Could not be experimentally determined.

mixture of toluene (20 mL), ethanol (7 mL) and 2 M Na<sub>2</sub>CO<sub>3</sub> (7 mL). The stirring solution was heated at reflux over a 24-h period. The cooled solution was extracted with ethyl acetate, washed with water and brine, and dried with MgSO<sub>4</sub>. Silica was added, and the slurry was concentrated to a solid to affect adhesion to the gel. This was chromatographed (silica, 5% ethyl acetate in hexanes) to yield a white solid, 4.4 g (74% yield): <sup>1</sup>H NMR (500 MHz, CDCl<sub>3</sub>)  $\delta$  (ppm): 6.95 (*m*, 1H), 7.01 (*m*, 1H), 7.41 (*m*, 1H), 7.61 (*d*, *J* = 5.0 Hz, 2H), 7.75 (*d*, *J* = 5.0 Hz, 2H); <sup>13</sup>C NMR (125 MHz, C-F coupled spectrum, CDCl<sub>3</sub>)  $\delta$  (ppm): 104.9 (*t*, *J* = 25.9 Hz), 111.6, 112.1 (*dd*, *J* = 3.7, 21.4 Hz), 118.8, 123.6 (*dd*, *J* = 3.9, 13.3 Hz), 129.7 (*d*, *J* = 3.2 Hz), 131.4 (*dd*, *J* = 4.4, 9.6 Hz), 132.4, 139.7, 160.0 (*dd*, *J* = 11.9, 252.1 Hz), 163.1 (*dd*, *J* = 12.0, 251.4 Hz); <sup>19</sup>F NMR (470 MHz, CDCl<sub>3</sub>)  $\delta$  (ppm): −112.0 (*m*, 3F), −116.2 (*m*, 3F).

### 3.1.2 2,4,6-tris(2',4'-difluoro-[1,1'-biphenyl]-4-yl)-1,3,5-triazine [tris-(dFB)Tz]

To a solution of TfOH (3 mL) in dry CHCl<sub>3</sub> (5 mL) at 0°C under argon was added a solution of 2',4'-difluoro-[1,1'-biphenyl]-4-carbonitrile (7.01 g, 3.26 × 10<sup>−2</sup> mol) in dry CHCl<sub>3</sub> (20 mL) dropwise over 5 min. The resulting red solution was heated to reflux for 18 h. The solution was cooled and poured into methanol, whereupon a white solid precipitated from solution. This was filtered off and rinsed alternately with liberal amounts of methanol and dichloromethane. Mass recovered: 5.98 g (85%). After 3 × train-style sublimations recovered mass decreased to 5.2 g; <sup>1</sup>H NMR (500 MHz, CDCl<sub>3</sub>)  $\delta$  (ppm): 6.99 (*m*, 3H), 7.04 (*m*, 3H), 7.55 (*m*, 3H), 7.75 (*d*, *J* = 7.2 Hz, 6H), 8.87 (*d*, *J* = 7.2 Hz, 6H).

## 3.2 Characterization of Tris-(dFB)Tz

The electronic properties of tris-(dFB)Tz, including  $\lambda_{\max}$  and  $E_{\text{LUMO}}$ , were evaluated and are shown in Table 1. The solution absorbance spectrum of tris-(dFB)Tz was measured in dichloromethane and the  $\lambda_{\max}$  found to be 305 nm, corresponding to an estimated optical bandgap of 3.66 eV, as seen in Fig. 2(a). Low-temperature delayed luminescence spectrum of tris-(dFB)Tz was collected at 77 K and compared to the phosphorescent blue emitter FIrpic [see Fig. 2(b)]. The phosphorescent spectrum of tris-(dFB)Tz is very broad without a well-defined 0–0 transition, making it difficult to define the triplet energy. But, by comparing the spectra, it is clear that the triplet energy of FIrpic is higher than tris-(dFB)Tz.

Cyclic voltammetry was used to estimate the  $E_{\text{LUMO}}$  of tris-(dFB)Tz. The first and second reduction potentials of tris-(dFB)Tz are 1.9 and 2.6 V, respectively (DMF, using ferrocene as an internal standard). From this data, the  $E_{\text{LUMO}}$  of tris-(dFB)Tz is estimated<sup>24</sup> to be −3.5 eV. Attempts to measure the oxidation potential, and thus  $E_{\text{HOMO}}$ , of tris-(dFB)Tz failed due to the poor solubility of the compound in dichloromethane.

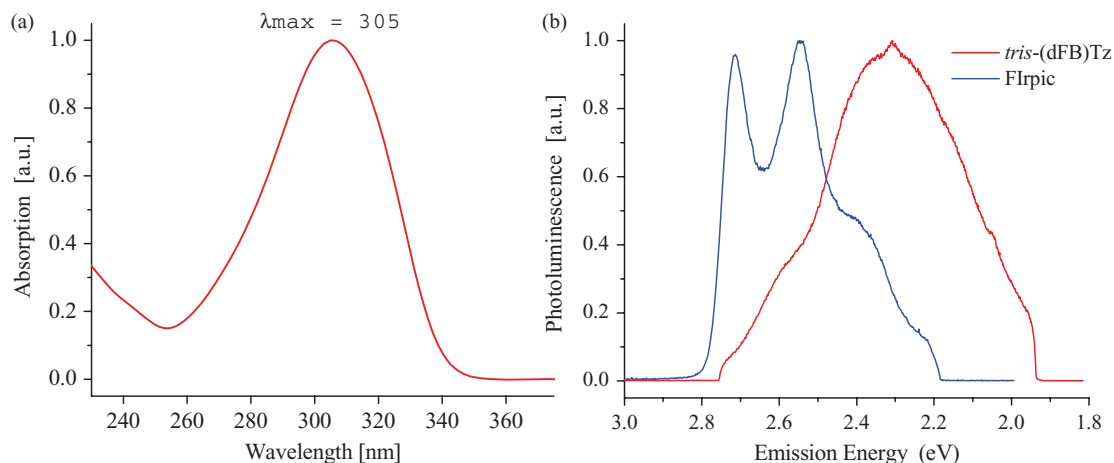


**Fig. 2** (a) Normalized absorbance spectrum of tris-(dFB)Tz (in dichloromethane at room temperature) and (b) normalized delayed luminescence spectra for tris-(dFB)Tz (red) and Flrpic (blue) measured in dichloromethane at 77 K.

### 3.3 Thin-Film Absorption

The absorption spectra of neat and 8 wt.%  $\text{Cs}_2\text{CO}_3$ -doped tris-(dFB)Tz films are shown in Fig. 3. There is no appreciable difference in the absorption spectra of the two films in the UV-Vis region. Any differences in emission intensity of an operating OLED when tris-(dFB)Tz is doped with  $\text{Cs}_2\text{CO}_3$  is therefore not a result of a change in the absorption properties of the tris-(dFB)Tz layer.

## 4 Results and Discussion

### 4.1 Electron-Only Devices—Demonstration of *n*-Doping in tris-(dFB)Tz

To demonstrate *n*-doping in tris-(dFB)Tz, electron-only devices were fabricated. Specifically, electron-only devices were made by depositing tris-(dFB)Tz neat or via codeposition with cesium carbonate ( $\text{Cs}_2\text{CO}_3$ ). The device architecture was ITO/200-Å Al/1000-Å tris-(dFB)Tz:*x* wt. %  $\text{Cs}_2\text{CO}_3$ /cathode, where *x* is 0 or 8% and cathode is 10-Å LiF/1000-Å Al or 1000-Å Al. The 200-Å layer of Al was deposited on the ITO surface to eliminate the possibility of

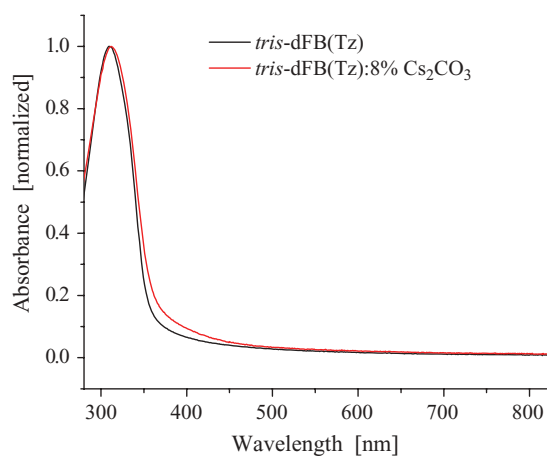


**Fig. 3** Normalized absorption spectra for neat tris-(dFB)Tz and tris-(dFB)Tz:8 wt.%  $\text{Cs}_2\text{CO}_3$ .

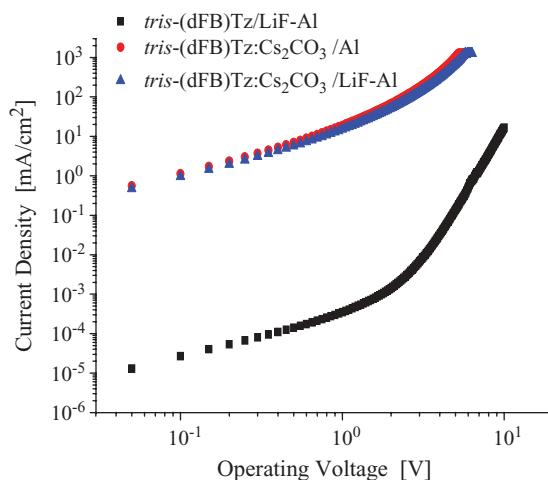


**Fig. 4** Electron-only devices for tris-(dFB)Tz with the following structure: ITO/200-Å Al/1000-Å tris-(dFB)Tz:*x* wt.% Cs<sub>2</sub>CO<sub>3</sub>/cathode, where *x* is 0 or 8% and cathode is 10-Å LiF/1000-Å Al or 1000-Å Al.

hole injection from ITO into tris-(dFB)Tz. The data in Fig. 4 show a significant increase in the current density for the doped devices compared to the undoped devices. The linear portion of the current density versus operation voltage ( $J$ - $V$ ) curves at low voltage, where  $J \propto V$  is satisfied is referred to as the ohmic region. Ohm's law states that  $J = Ne\mu V/t$ , where  $J$  is current density,  $N$  is the concentration of charge carriers (electron in this case),  $e$  is the charge of an electron,  $\mu$  is the electron mobility,  $V$  is the applied voltage, and  $t$  is the thickness of the organic layer (1000 Å, in this case);  $V/t$  equals the electric field. From the preceding equation, assuming unchanged mobility, the  $J$ - $V$  plots in Fig. 4 can be used to calculate the increase in the number of electrons by determining the current-density change between the two ohmic regimes for undoped and doped tris-(dFB)Tz. Thus, we measure the carrier concentration of the tris-(dFB)Tz films to increase by four orders of magnitude on doping with Cs<sub>2</sub>CO<sub>3</sub>.

To achieve good electron injection from Al into undoped ETMs, an electron injection layer of an alkali halide or alkaline earth halide is often deposited at the ETL-cathode interface.<sup>31–33</sup> Undoped tris-(dFB)Tz required this electron injection layer (data not shown). Doped tris-(dFB)Tz devices, however, did not require an interfacial electron injection layer, as shown in Fig. 4. Devices fabricated with and without LiF at the ETL-cathode interface show identical behavior. The data in Fig. 4 indicate that when tris-(dFB)Tz is doped with Cs<sub>2</sub>CO<sub>3</sub>, an ohmic contact forms.

## 4.2 Blue Phosphorescent OLED Results

Once the ability of Cs<sub>2</sub>CO<sub>3</sub>-doped tris-(dFB)Tz to improve both the interfacial electron injection and bulk conductivity was established, the materials were evaluated in blue phosphorescent OLEDs. The blue phosphorescent OLEDs were fabricated using *N,N'*-bis(naphthalen-1-yl)-*N,N'*-bis(phenyl)-benzidine (NPD) as the hole-transporting layer, 4,4',4''-tris(carbazol-9-yl)triphenylamine (TCTA) as the electron- and exciton-blocking layer, 4-(diphenylphosphoryl)-*N,N*-diphenylaniline (HM-A1) as the host in the emissive layer, iridium(III)bis[(4,6-difluorophenyl)-pyridinato-*N,C*']picolinate (FIrpic) as the phosphorescent emitter in the emissive layer, and bis(diphenylphosphoryl)dibenzothiophene (PO15) and/or tris-(dFB)Tz as the ETM. In Fig. 5, we show device data for OLEDs with the following architecture: ITO/350-Å NPD/50-Å TCTA/150-Å HM-A1:5%FIrpic/500-Å ETL/10-Å LiF/1000-Å Al, where ETL

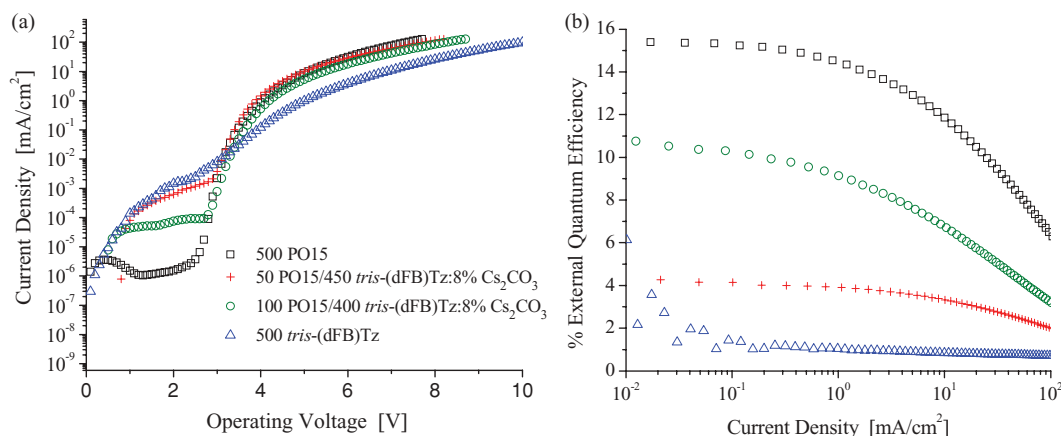


**Fig. 5** (a) Current density versus drive voltage and (b) EQE versus current density for blue phosphorescent OLEDs with the following architecture: ITO/300-Å NPD/50-Å TCTA/150-Å HM-A1:5%Flrpic/500-Å ETL/10Å LiF/1000-Å Al, where ETL was 500-Å PO15 (black), 50-Å PO15/450 tris-(dFB)Tz:8% Cs<sub>2</sub>CO<sub>3</sub> (red), 100-Å PO15/400 tris-(dFB)Tz:8% Cs<sub>2</sub>CO<sub>3</sub> (green), and 500 tris-(dFB)Tz (blue).

was 500-Å PO15 (black), 50-Å PO15/450 tris-(dFB)Tz:8% Cs<sub>2</sub>CO<sub>3</sub> (red), 100-Å PO15/400 tris-(dFB)Tz:8% Cs<sub>2</sub>CO<sub>3</sub> (green), and 500 tris-(dFB)Tz (blue).

OLEDs with 500-Å PO15 had a operating voltage of  $4.05 \pm 0.02$  V and an external quantum efficiency (EQE) of  $14.5 \pm 0.5\%$ , while the OLEDs with 500-Å tris-(dFB)Tz had a operating voltage of  $5.05 \pm 0.02$  V and an EQE of  $1.03 \pm 0.02\%$ . The significant drop in EQE was expected due to the fact that tris-(dFB)Tz has a lower triplet energy than Flrpic [see Fig. 2(b)], which leads to excitons transferring onto the ETL material and being subsequently quenched. These results indicate that a high triplet energy buffer layer must be inserted between tris-(dFB)Tz and the emissive layer in order to obtain high EQE for blue OLEDs (see in the following). By comparing OLEDs with either PO15 or tris-(dFB)Tz as the ETL [see Fig. 5(a)], insight is gained into how tris-(dFB)Tz influences drive voltage in comparison to PO15. We believe the higher operating voltage for the tris-(dFB)Tz devices is due to both the larger injection barrier for electrons from tris-(dFB)Tz ( $E_{\text{LUMO}} = -3.52$  eV) into HM-A1 ( $E_{\text{LUMO}} = -2.56$ ) and lower electronic conductivity of tris-(dFB)Tz films.

To ascertain whether a device incorporating a high triplet energy buffer layer between the emissive layer and the tris-(dFB)Tz ETL would improve EQE, we fabricated and tested blue phosphorescent OLEDs using a 50- and 100-Å thick PO15 ( $E_T = 3.1$  eV) buffer layers. As seen in Fig. 5(b), significant quenching still existed when the 50-Å buffer layer was inserted. Increasing the thickness of the buffer layer to 100 Å resulted in less quenching of the triplet exciton and a significant increase in EQE, but EQE was still lower than the PO15-only control device. Because the  $J$ - $V$  curves of devices with different thicknesses of PO15 buffer layer are nearly identical to that of the PO15-only control device, the low EQE of devices with a PO15-tris-(dFB)Tz ETL combination is not due to reduced charge injection or lower electron conductivity. It is possible that even thicker buffer layers could be employed to maximize EQE without causing a significant change in operating voltage.

### 4.3 Influence of ETL Thickness on Operating Voltage

One of the main advantages of doped ETLs compared to undoped ETLs is that thicker layers can be utilized without significantly increasing the device operating voltage. Thicker transport layers may be useful in two ways. First, there is some evidence that the surface plasmon excitation in the reflective cathode is responsible for a portion of light lost internally in the OLED and

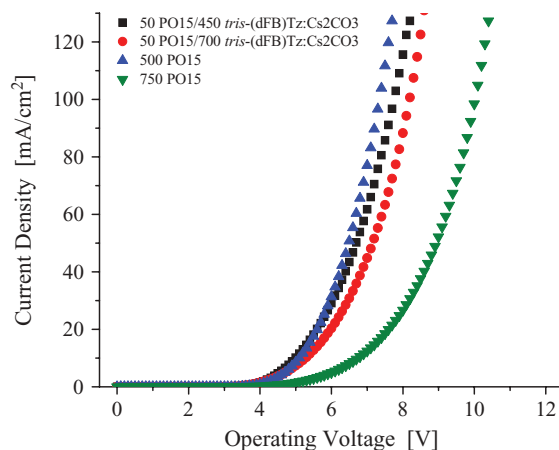


**Fig. 6** Current density versus drive voltage for devices with different ETL thicknesses: ITO/300-Å NPd/50-Å TCTA /150-Å HM-A1:5% Firpic/ETL/1000-Å Al, where ETL is 50-Å PO15/450 tris-(dFB)Tz:8% Cs<sub>2</sub>CO<sub>3</sub> (black), 50-Å PO15/700-Å tris-(dFB)Tz:8% Cs<sub>2</sub>CO<sub>3</sub> (red), 500-Å PO15/10-Å LiF (blue), or 750-Å PO15/10-Å LiF (green).

that this loss can be mitigated by increasing the distance between the emissive layer and the cathode<sup>34,35</sup>. Second, thicker charge transport layers may provide a wider process window, which can improve the manufacturability of OLEDs and increase device yields. In Fig. 5, we show results for a fixed ETL thickness of 500 Å. At this thickness, the doped tris-(dFB)Tz devices had the same  $J$ - $V$  characteristic as the undoped PO15 devices. Hence, a operating voltage advantage is not observed when going from the undoped PO15 to the doped tris-(dFB)Tz film because PO15 has a high-enough electron mobility that the voltage drop across the 500-Å PO15 ETL does not significantly raise the operating voltage.

Figure 6 shows  $J$ - $V$  curves for devices with different ETL thicknesses: ITO/300-Å NPd/50-Å TCTA /150-Å HM-A1:5% Firpic/ETL/1000-Å Al, where ETL is 50-Å PO15/450 tris-(dFB)Tz:8% Cs<sub>2</sub>CO<sub>3</sub> (black), 50-Å PO15/700-Å tris-(dFB)Tz:8% Cs<sub>2</sub>CO<sub>3</sub> (red), 500-Å PO15/10-Å LiF (blue), or 750-Å PO15/10-Å LiF (green). Of particular note is that there is a significant increase in operating voltage for a PO15 device when the ETL thickness is increased from 500 to 700 Å. However, the operating voltage of the 700-Å tris-(dFB)Tz:8% Cs<sub>2</sub>CO<sub>3</sub> device is much closer to the devices with a 500-Å-thick ETL due to the high conductivity provided by the electronic doping. This demonstrates the potential utility of conductivity doping in permitting the use of thicker charge transport layers.

## 5 Conclusion

We reported a high-yielding alternative synthesis, photophysical properties, and electrochemical characterization of tris-(dFB)Tz. The deep LUMO energy of tris-(dFB)Tz makes it an attractive candidate for use as an electron acceptor in an  $n$ -doped electron transport layer. Tris-(dFB)Tz films doped with Cs<sub>2</sub>CO<sub>3</sub> show a 10,000-fold increase in the number of carriers relative to undoped films. Additionally, an ohmic contact between tris-(dFB)Tz and the aluminum cathode forms on doping with Cs<sub>2</sub>CO<sub>3</sub>. We reported the first OLEDs utilizing tris-(dFB)Tz as an  $n$ -doped electron transport layer. The OLEDs with  $n$ -doped tris-(dFB)Tz ETLs have lower operating voltages than OLEDs with the high-performance electron transport layer PO15 when thick (700-Å) transport layers are used, emphasizing the advantage of doped transport layers over undoped transport layers when thick device stacks are desired. These new results with tris-(dFB)Tz suggest that other aromatic substituted triazines could also function as  $n$ -doped electron transport layers in OLEDs and other organic electronic devices.

## Acknowledgments

This project was funded by the Solid State Lighting Program of the U.S. Department of Energy (US DOE), within the Building Technologies Program (Award No. M6743231, managed by the National Energy Technology Laboratory). A portion of this research was performed using the Environmental Molecular Science Laboratory, a national scientific user facility sponsored by the Department of Energy's Office of Biological and Environmental Research and located at Pacific Northwest National Laboratory (PNNL). Computations were performed using NWChem, a computational chemistry package for parallel computers, version 5.1 (2007), which was developed at the High Performance Computational Chemistry Group, PNNL, Richland, Washington. PNNL is operated by Battelle Memorial Institute for the US DOE (under Contract No. DE\_AC06–76RLO 1830).

## References

1. K. Walzer, B. Maennig, M. Pfeiffer, and K. Leo, "Highly efficient organic devices based on electrically doped transport layers," *Chem. Rev.* **107**, 1233–1271 (2007).
2. M. Pfeiffer, K. Leo, X. Zhou, J. Huang, M. Hofmann, A. Werner, and J. Blochwitz-Nimoth, "Doped organic semiconductors: physics and application in light emitting diodes," *Org. Electron.* **4**, 89–103 (2003).
3. R. Meerheim, B. Lussem, and K. Leo, "Efficiency and stability of p-i-n type organic light emitting diodes for display and lighting applications," *Proc. IEEE* **97**, 1606–1626 (2009).
4. W. Gao and A. Kahn, "Electrical doping: the impact on interfaces of  $\pi$ -conjugated molecular films," *J. Phys. Condens. Matter.* **15**, S2757–S2770 (2003).
5. J. Kido and T. Matsumoto, "Bright organic electroluminescent devices having a metal-doped electron-injecting layer," *Appl. Phys. Lett.* **73**, 2866–2868 (1998).
6. G. Parthasarathy, C. Adachi, P. E. Burrows, and S. R. Forrest, "High-efficiency transparent organic light-emitting devices," *Appl. Phys. Lett.* **76**, 2128–2130 (2000).
7. G. Parthasarathy, C. Shen, A. Kahn, and S. R. Forrest, "Lithium doping of semiconducting organic charge transport materials," *J. Appl. Phys.* **89**, 4986–4992 (2001).
8. J. Huang, M. Pfeiffer, A. Werner, J. Blochwitz, K. Leo, and S. Liu, "Low-voltage organic electroluminescent devices using pin structures," *Appl. Phys. Lett.* **80**, 139–141 (2002).
9. G. He, O. Schneider, D. Qin, X. Zhou, M. Pfeiffer, and K. Leo, "Very high-efficiency and low voltage phosphorescent organic light-emitting diodes based on a p-i-n junction," *J. Appl. Phys.* **95**, 5773–5777 (2004).
10. T. Matsushima and C. Adachi, "Extremely low voltage organic light-emitting diodes with p-doped alpha-sexithiophene hole transport and n-doped phenyldipyrenylphosphine oxide electron transport layers," *Appl. Phys. Lett.* **89**, 253506 (2006).
11. T. Oyamada, C. Maeda, H. Sasabe, and C. Adachi, "Efficient electron injection characteristics of tetra-2-pyridinylpyrazine (TPP) in organic light emitting diodes," *Chem. Lett.* **32**, 388–389 (2003).
12. T. Hasegawa, S. Miura, T. Moriyama, T. Kimura, I. Takaya, Y. Osato, and H. Mizutani, "11.3: novel electron-injection layers for top-emission OLEDs," *SID Symp. Dig. Tech. Papers* **35**, 154–157 (2004).
13. C.-I. Wu, C.-T. Lin, Y.-H. Chen, M.-H. Chen, Y.-J. Lu, and C.-C. Wu, "Electronic structures and electron-injection mechanisms of cesium-carbonate-incorporated cathode structures for organic light-emitting devices," *Appl. Phys. Lett.* **88**, 152104 (2006).
14. T.-W. Lee, T. Noh, B.-K. Choi, M.-S. Kim, D. W. Shin, and J. Kido, "High-efficiency stacked white organic light-emitting diodes," *Appl. Phys. Lett.* **92**, 043301 (2008).
15. Y. Z. Li, G. Z. Ran, W. Q. Zhao, and G. G. Qin, "Au generation centres doped n(+)-Si: hole-injection adjustable anode for efficient organic light emission," *J. Phys. D* **41**, 155107 (2008).

16. T. Park, S. Kim, W. Jeon, J. Park, R. Pode, J. Jang, and J. Kwon, “Electrical characterization of N- and P-doped hole and electron only organic devices,” *J. Nanosci. Nanotechnol.* **8**, 5606–5609 (2008).
17. M.-H. Chen, D.-S. Leem, C. T. Lin, G. R. Lee, T.-W. Pi, J.-J. Kim, and C.-I. Wu, “Investigations of electron-injection mechanisms and interfacial chemical reactions of Bphen doped with rubidium carbonate in OLEDs,” *Proc. SPIE* **7051**, 70511C (2008).
18. D.-S. Leem, S.-Y. Kim, J.-J. Kim, M.-H. Chen, and C.-I. Wu, “Rubidium-carbonate-doped 4,7-diphenyl-1,10-phenanthroline electron transporting layer for high-efficiency p-i-n organic light emitting diodes,” *Electrochem. Solid-State Lett.* **12**, J8–J10 (2009).
19. M. Khan and W. Xu, “Highly power efficient organic light-emitting diodes based on p-doped and novel n-doped carrier transport layers,” *J. Phys. D* **40**, 6535–6540 (2007).
20. W. Xu, M. Khan, Y. Bai, X. Jiang, Z. Zhang, and W. Zhu, “High-efficiency pin organic light-emitting diodes with a novel n-doping electron transport layer,” *Curr. Appl. Phys.* **9**, 732–736 (2009).
21. V.-E. Choong, S. Shi, J. Curless, and F. So, “Bipolar transport organic light emitting diodes with enhanced reliability by LiF doping,” *Appl. Phys. Lett.* **76**, 958–960 (2000).
22. K. R. Choudhury, J. H. Yoon, and F. So, “LiF as an n-dopant in tris(8-hydroxyquinoline) aluminum thin films,” *Adv. Mater.* **20**, 1456–1461 (2008).
23. J. Birnstock, A. Lux, M. Ammann, P. Wellmann, M. Hofmann, and T. Stubinger, “64.4: novel materials and structures for highly-efficient, temperature-stable, and long-living AM OLED displays,” *SID Symp. Dig. Tech. Papers* **37**, 1866–1869 (2006).
24. D. Kolosov, V. Adamovich, P. Djurovich, M. E. Thompson, and C. Adachi, “1,8-naphthalimides in phosphorescent organic LEDs: the interplay between dopant, exciplex, and host emission,” *J. Am. Chem. Soc.* **124**, 9945–9954 (2002).
25. N. J. Turro, *Modern Molecular Photochemistry*, Chap. 5, University of Science Books, Sausalito, CA, pp. 146–148 (1991).
26. E. J. Bylaska, W. A. de Jong, N. Govind, K. Kowalski, T. P. Straatsma, M. Valiev, D. Wang, E. Apra, T. L. Windus, J. Hammond, P. Nichols, S. Hirata, M. T. Hackler, Y. Zhao, P.-D. Fan, R. J. Harrison, M. Dupuis, D. M. A. Smith, J. Nieplocha, V. Tipparaju, M. Krishnan, Q. Wu, T. Van Voorhis, A. A. Auer, M. Nooijen, L. D. Crosby, E. Brown, C. Cisneros, G. I. Fann, H. Fruchtl, J. Garza, K. Hirao, R. Kendall, J. A. Nichols, K. Tsemekhman, K. Wolinski, J. Anchell, D. Bernholdt, P. Borowski, T. Clark, D. Clerc, H. Dachsel, M. Deegan, K. Dylla, D. Elwood, E. Glendening, M. Gutowski, A. Hess, J. Jaffe, B. Johnson, J. Ju, R. Kobayashi, R. Kutteh, Z. Lin, R. Littlefield, X. Long, B. Meng, T. Nakajima, S. Niu, L. Pollack, M. Rosing, G. Sandrone, M. Stave, H. Taylor, G. Thomas, J. van Lenthe, A. Wong, and Z. Zhang, *NWChem, A Computational Chemistry Package for Parallel Computers, Version 5.1*, Pacific Northwest National Laboratory, Richland, WA (2008).
27. R. A. Kendall, E. Aprà, D. E. Bernholdt, E. J. Bylaska, M. Dupuis, G. I. Fann, R. J. Harrison, J. Ju, J. A. Nichols, J. Nieplocha, T. P. Straatsma, T. L. Windus, and A. T. Wong, “High performance computational chemistry: an overview of NWChem a distributed parallel application,” *Comput. Phys. Commun.* **128**, 260–283 (2000).
28. T. Ishi-i, K. Yaguma, T. Thiemann, M. Yashima, K. Ueno, and S. Mataka, “High electron drift mobility in an amorphous film of 2, 4, 6,-tris [4-(1-naphthyl) phenyl]-1, 3, 5-triazine,” *Chem. Lett.* **33**, 1244–1245 (2004).
29. J. Pang, Y. Tao, S. Freiberg, X. P. Yang, M. D’Iorio, and S. N. Wang, “Syntheses, structures, and electroluminescence of new blue luminescent star-shaped compounds based on 1,3,5-triazine and 1,3,5-trisubstituted benzene,” *J. Mater. Chem.* **12**, 206–212 (2002).
30. A. Ranganathan, B. C. Heisen, and I. D. F. Meyer, “A triazine-based three-directional rigid-rod tecton forms a novel 1D channel structure,” *Chem. Commun.* 3637–3639 (2007).
31. D. Y. Kondakov, “Voltammetric study of Bphen electron-transport layer in contact with LiF/Al cathode in organic light-emitting diodes,” *J. Appl. Phys.* **99**, 024901–024904 (2006).

32. L. S. Hung and S. T. Lee, "Electrode modification and interface engineering in organic light-emitting diodes," *Mater. Sci. Eng., B* **85**, 104–108 (2001).
33. L. S. Hung, C. W. Tang, and M. G. Mason, "Enhanced electron injection in organic electroluminescence devices using an Al/LiF electrode," *Appl. Phys. Lett.* **70**, 152–154 (1997).
34. P. A. Hobson, J. A. E. Wasey, I. Sage, and W. L. Barnes, "The role of surface plasmons in organic light-emitting diodes," *IEEE J. Select. Top. Quantum Electron.* **8**, 378–386 (2002).
35. B. C. Krummacher, S. Nowy, J. Frischeisen, M. Klein, and W. Brütting, "Efficiency analysis of organic light-emitting diodes based on optical simulation," *Org. Electron.* **10**, 478–485 (2009).